



Beamline: ID11	Experiment title: Unravelling the role of force chains in localised shearing of granular materials	Experiment number: ma3373
Shifts: 12	Date of experiment: from: 19 May 2017 to: 23 May 2017 Local contact(s): Marta Majkut	Date of report: <i>Received at ESRF:</i>
Names and affiliations of applicants (* indicates experimentalists): Stephen Hall ^{*,1} , Ryan Hurley ^{*,2,3} , Eric Herbold ^{*,2} , Jonas Engqvist ¹ ¹ Division of Solid Mechanics, Lund University, Sweden. ² Lawrence Livermore National Laboratory, Livermore, CA, USA. ³ Johns Hopkins University, Baltimore, MD, USA.		

Report:

The primary goal of experiment ma3373 at ID11 was to investigate the localised shearing behavior of granular samples subjected to triaxial stress conditions. To accomplish this goal, several granular materials composed of spherical ruby grains and angular quartz grains were subjected to uniaxial stress conditions using a custom-built load frame (also used in ma1913 and ma2665), and triaxial stress conditions using a new custom-built load frame (shown in Fig. 1). The new load frame possesses an actuator-driven load piston, a fluid-filled pressure cell, and a pressure-controlled pump. 3DXRD and x-ray tomography, developed and used for granular materials in prior experiments at ID11 (ma828, ma1216, ma1913, ma2665, [1-6]), were successfully used in all experiments to make high-resolution measurements of structure, contacts, pore space, and grain-averaged stress tensors. Ultrasound measurements were made simultaneously with some of the samples subjected to uniaxial stress conditions to understand the changes in transport properties that occur during localised shearing or grain fracture. The experiments represent the first time that shear localisation in granular materials has been experimentally studied with 3DXRD, which uniquely permits quantifying the grain stress tensors and the inter-grain contact force network (see ma1913 [3]).

Experiment and measurement. – Four granular samples were investigated in uniaxial or triaxial stress conditions (see Fig. 1b-e): (1) 877 spherical single-crystal ruby grains, diameter 135 microns, uniaxial stress; (2) 886 spherical single-crystal ruby grains, diameter 135 microns, triaxial stress; (3) 243 single-crystal angular quartz grains, triaxial stress; (4) 22 spherical single-crystal quartz grains, diameter 450 microns, uniaxial stress. The latter sample was briefly studied to test one new feature of the custom-built uniaxial load frame: ultrasound transducers and receivers to quantify wave transport through the packing. All samples were placed in the appropriate load frame and compressed by an actuator-driven piston to a desired sample strain level. Upon reaching the desired sample strain level, the sample was rotated 180° to obtain 1800

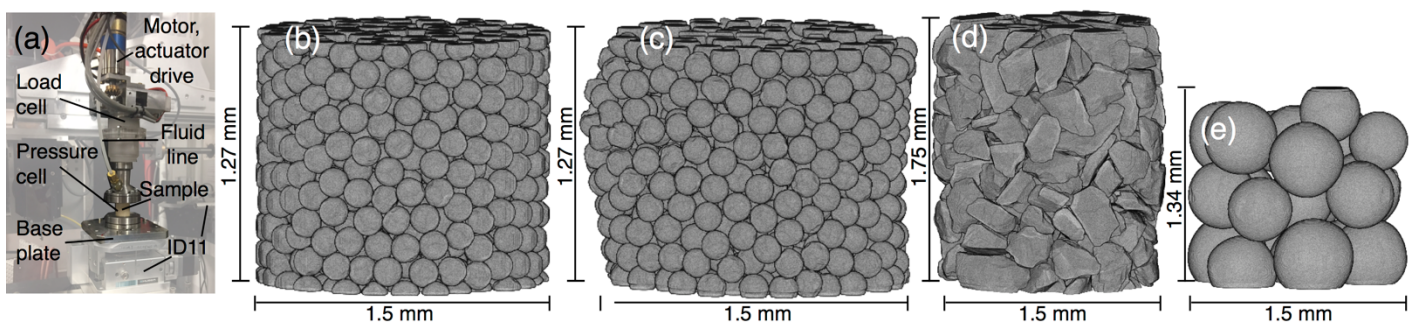


Figure 1 - (a) Custom triaxial load frame. (b) 877 ruby grains in uniaxial compression. (c) 876 ruby grains in triaxial compression. (d) 243 quartz grains in triaxial compression. (e) 22 quartz spheres in uniaxial compression with ultrasound.

transmission radiographs at 0.1° angle increments and 360° to obtain 1440 diffraction patterns at 0.25° increments. Loading and measurements were repeated in a sequence until load cell readings indicated significant sample softening (negative overall slope of the force-displacement curve), grain fracture was evident in transmission radiographs, or significant localised deformation was observed in transmission radiographs and fast tomogram reconstructions using pyHST2 (described below). The number of load steps for samples 1 through 4 was 13, 15, 6, and 5, respectively.

Results and analysis. – We performed X-ray computed tomography (XRCT) reconstructions using pyHST2 and morphological grain segmentation (e.g. Figs.

1b-e) using methods developed in [3,4]. Processing of diffraction data using methods from [7] is currently ongoing. Analysis of grain kinematics has been performed for experiments (1), (2), and (4), and is in progress for sample (3) but is more complex due to significant grain rotations and grain fracture. Grain kinematics for sample (2) have been analyzed, used to compute equivalent continuum-equivalent strain fields, and presented at conferences to the granular mechanics community [6,8,9]. Figure 2 illustrates these grain kinematics and continuum-equivalent strain fields. Grain characteristics from sample (3) have been analyzed with bounding box algorithms, used to complement a separate study [10], and used to create particle meshes for 3D finite-element simulations. Ongoing analysis includes:

- 3DXRD of samples (1) and (2) is currently being performed to determine grain-resolved stress tensors and crystal orientations. Side-by-side analysis of the resulting grain-resolved stress tensors for samples (1) and (2), in combination with XRCT data, will be used with force-inference methods from [3] to understand how grain stresses and force chains evolve inside of shear bands, and how the general statistics and structure of force networks differ between samples that do and do not contain shear localisation. Side-by-side analysis of crystal orientations for samples (1) and (2) will be used to investigate how local relative grain rotations differ in samples with and without shear localisation, and to investigate higher-order continua (e.g. micromorphic) descriptions of granular media.
- 3DXRD data for sample (3) is currently being performed to determine grain-resolved stress tensors and crystal orientations. This data, in combination with XRCT data for sample (3), will provide information about the interrelationship between grain fracture, grain stresses, and shear localisation in granular materials, and will be used to calibrate 3D finite-element simulations employing continuum damage mechanics models.
- XRCT and 3DXRD data for sample (4) is currently being processed and will be used to develop experiments for testing the transport properties of granular materials in the near future, and for developing non-destructive procedures for evaluating the presence of shear localisation based on changes in ultrasound transmission.

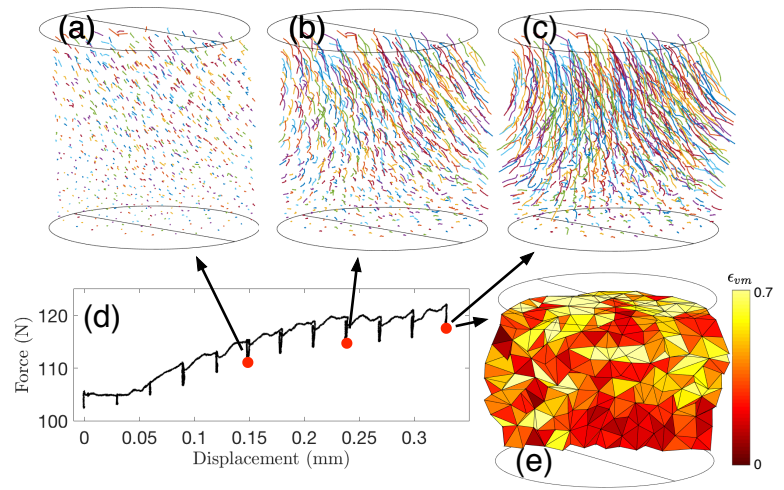


Figure 2 – (a)-(c) grain kinematics for sample (2) at load steps 6, 10, and 14. (d) Force-displacement from load cell and load piston motion. (e) von Mises strain in grain-centered mesh at load step 14.

[1] Hall, S.A., & Wright, J., (2014). *16th Int. Conf. Exp. Mech.*, Cambridge, UK.

[2] Hall, S.A., & Wright, J., (2015). *Geotechnique Lett.*, 5(4), 236-242.

[3] Hurley, R.C., Hall, S.A., Andrade, J.E., & Wright, J., (2016). *Phys. Rev. Lett.*, 117, 098005.

[4] Hurley, R.C., Hall, S.A., & Wright, J. (2017). *Proc. Royal Soc. A*, 473, 2207.

[5] Hurley, R.C., Hall, S.A., Andrade, J.E., & Wright, J., (2017). *EPJ Web of Conf.*, 140, 02006.

[6] Hall, S.A., Hurley, R.C., Wright, J., & Athanasopoulos, S., (2017). *ICTMS 2017*, 187.

[7] Oddershede, J., Schmidt, S., Poulsen, H.F., Sorensen, H.O., Wright, J., & Reimers, W., (2010). *J. Appl. Cryst.*, 43(3), 539-549.

[8] Hurley, R.C., (2017). *CHESS Users' Meeting*, Ithaca, NY, USA.

[9] Hurley, R.C., Herbold, E.B., Pagan, D.C., Hall, S.A., Wright, J., Lind, J., & Akin, M.C., (2017). *Society of Engineering Science, Annual Meeting*, Boston, MA, USA.

[10] Hurley, R.C., Herbold E.B., & Pagan, D.C., (2018). *J. Appl. Cryst.*, In Review.